



Abstract

- Internal (gravity) waves propagate through stratified fluid, vertically transporting horizontal momentum and thereby influencing mean atmospheric winds such as the QBO and, consequently, weather and climate.
- Internal waves were thought to be excited by the vertically fluctuating motion of the cloud tops when a strong convective system impinges upon the base of the stratosphere (Fritts and Alexander, 2003).
- This was drawn into question by laboratory experiments of a buoyant plume impinging upon a stratified fluid layer (Ansong and Sutherland, 2010) which showed that the frequency of internal waves emanating from the plume was narrow and not related to the broad-banded spectrum associated with fluctuations of the turbulent/non-turbulent (T/NT) interface of the fountain top.
- Inspired by these experiments, we perform 3D large eddy simulations of a buoyant plume impinging upon a stably stratified layer whose stratification strength ranges over two orders of magnitude between different simulations. We show that the waves originate from within the turbulent flow rather than at the T/NT interface.

Idealised numerical simulations

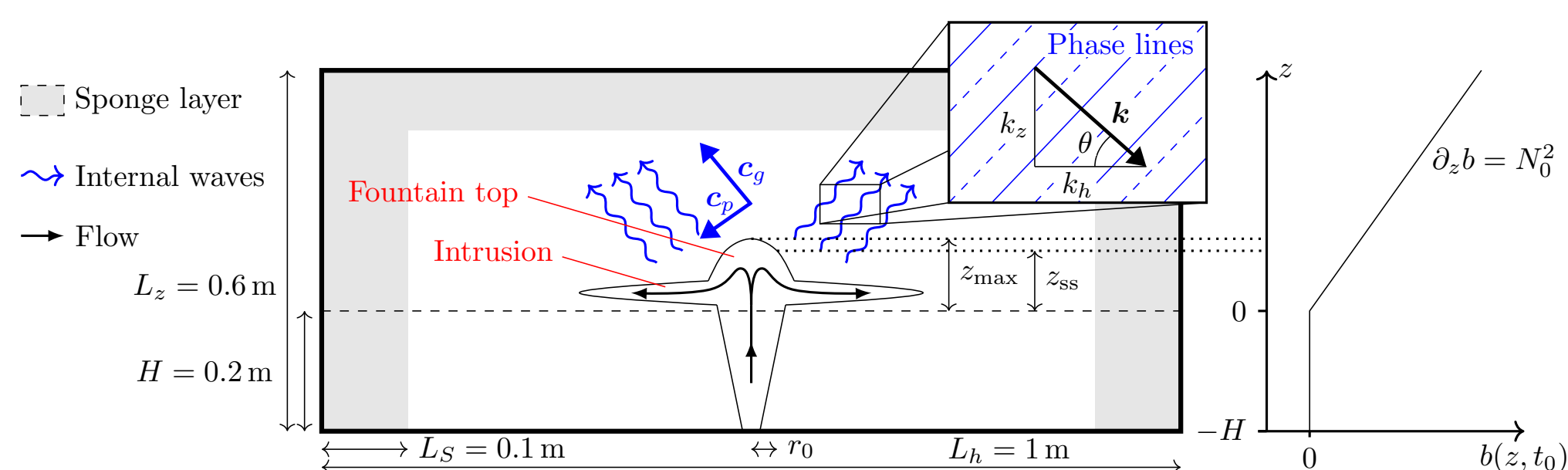


Figure 1. Simulation setup and key parameters.

- We consider a plume with integral vertical buoyancy flux F_0 and radius r_0 at the source.
- During penetration into the stably stratified layer, with $\partial_z b = N_0^2$, the plume transforms into a fountain that excites internal waves above, with collapsing fluid from the fountain spreading laterally as an intrusion at its neutral buoyancy level.
- Three moderate resolution simulations (512^3 grid) with $N_0^2 = 1, 10, 100 \text{ s}^{-2}$ and one high resolution simulation (1024^3 grid) with $N_0^2 = 0.25 \text{ s}^{-2}$ are first run until the wavefield has developed, then run for a further 6 (moderate res.) or 10 (high res.) buoyancy periods $T_b = 2\pi/N_0$.

Plume and wavefield evolution

- Internal waves appear to emanate from the fountain top and propagate outwards and upwards, forming concentric rings when viewed from above.

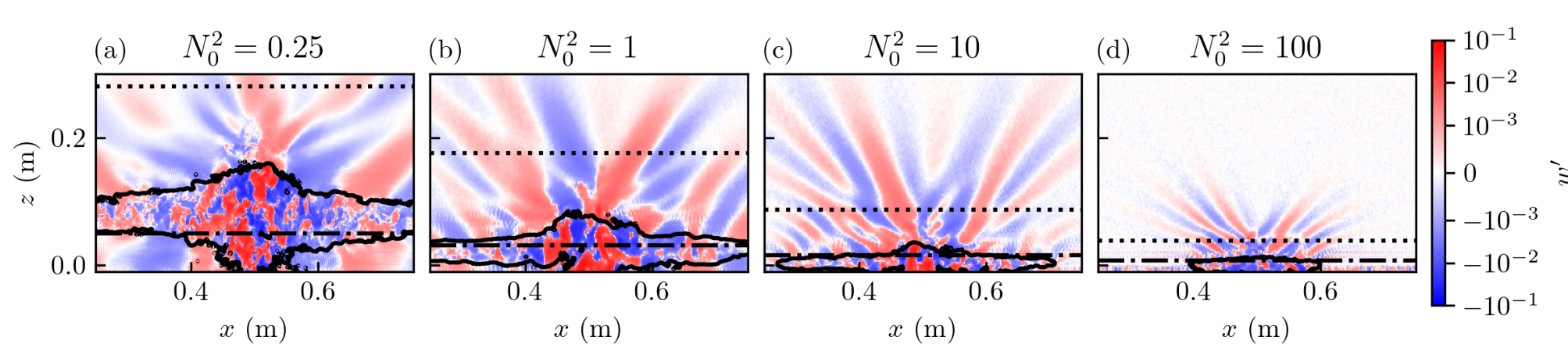


Figure 2. Vertical slices through the plume centreline, showing the turbulent vertical velocity w' . Spectra shown in figure 3 are calculated at $z/z_{\max} = 0.25$ (dot-dashed line) or $z/z_{\max} = 1.4$ (dotted line).

- Energy within the turbulent plume is two orders of magnitude larger than in the stratified ambient (figure 3b). The characteristic horizontal wavenumber $k_{h,c} \propto N_0^{0.5 \pm 0.05}$ (figure 3c).
- The characteristic wave frequency ω_c above the plume is an approximately fixed fraction of N_0 and there is no relationship between the plume and wave oscillation frequencies (figure 3d and 3e), consistent with laboratory experiments (Ansong and Sutherland, 2010).

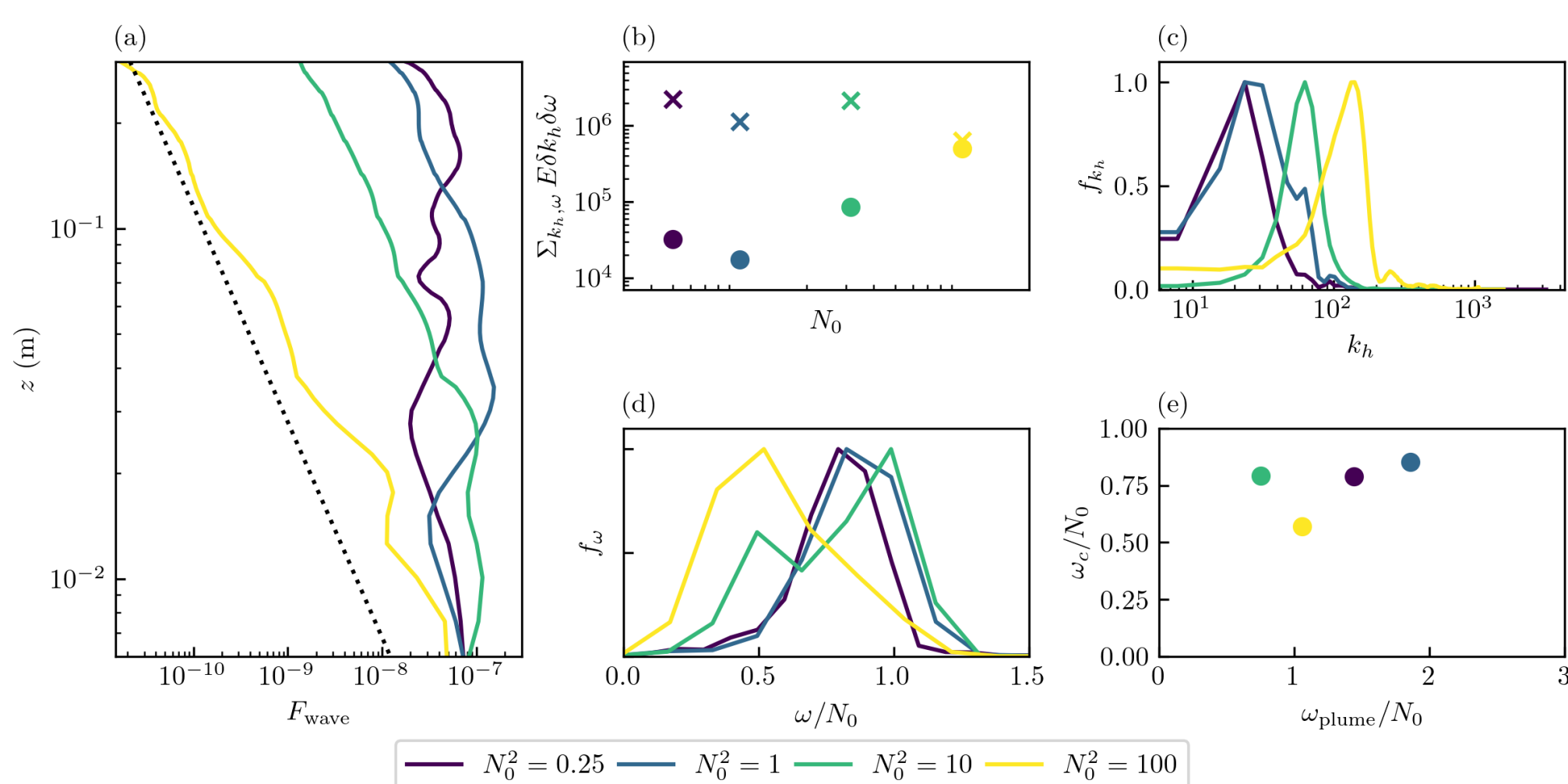


Figure 3. (a) Time-averaged vertical energy flux with strongly-stratified theoretical prediction (Couston et al., 2018) (black dotted line). (b) Total energy at $z/z_{\max} = 0.25, 1.4$ (crosses, circles). (c) Horizontal wavenumber spectrum f_{k_h} and (d) frequency spectrum f_{ω} at $z/z_{\max} = 1.4$. (e) Comparison of characteristic wave frequency ω_c and characteristic oscillation frequency of the turbulent/non-turbulent interface ω_{plume} .

References

- J. K. Ansong and B. R. Sutherland. Internal gravity waves generated by convective plumes. *J. Fluid Mech.*, 648:405–434, 2010. doi: 10.1017/S002211200993193.
- Louis-Alexandre Couston, Daniel Lecoanet, Benjamin Favier, and Michael Le Bars. The energy flux spectrum of internal waves generated by turbulent convection. *J. Fluid Mech.*, 854:R3, November 2018. doi: 10.1017/jfm.2018.669.
- David C. Fritts and M. Joan Alexander. Gravity wave dynamics and effects in the middle atmosphere. *Reviews of Geophysics*, 41(1): 2001RG000106, March 2003. doi: 10.1029/2001RG000106.
- Peter J. Schmid. Dynamic mode decomposition of numerical and experimental data. *J. Fluid Mech.*, 656:5–28, August 2010. doi: 10.1017/S0022112010001217.
- John R. Taylor and Sutanu Sarkar. Internal gravity waves generated by a turbulent bottom Ekman layer. *J. Fluid Mech.*, 590:331–354, November 2007. doi: 10.1017/S0022112007008087.

Spectral analysis

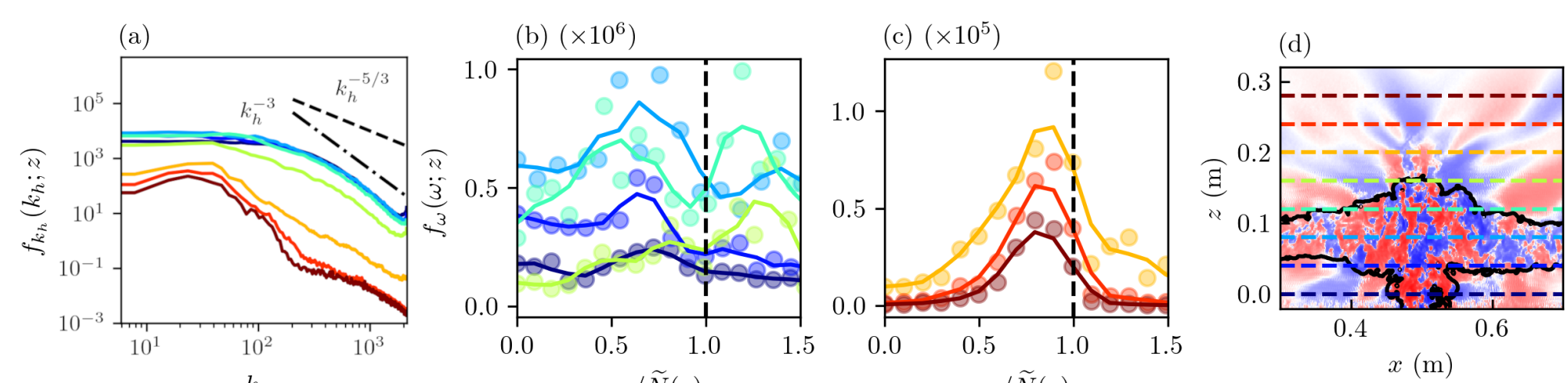


Figure 4. (a) Wavenumber spectrum f_{k_h} and (b), (c) frequency spectrum f_{ω} at a range of heights in the high resolution simulation with $N_0^2 = 0.25$, indicated by coloured lines in (d).

- Wavenumber spectra show an axisymmetric turbulence scaling k_h^{-3} within the plume (figure 4a).
- Frequency spectra are flat within the plume (figure 4b) and peaked above the plume (figure 4c), indicating selection of a range of frequencies close to, but below, N_0 .

Viscous internal wave model

- The observed frequency selection can be explained using a linear viscous decay model derived from Taylor and Sarkar (2007). Given wave amplitudes $A(k_h, \omega; z_0)$ at a height z_0 , predicted amplitudes $A^*(k_h, \omega; z)$ are calculated from vertical profiles of the time- and horizontal-average stratification \tilde{N}^{plume} (within the plume) and turbulent viscosity $\tilde{\nu}_{\text{tot}}$, shown in figure 5, according to

$$\frac{A^*(\omega, k_h; z)}{A(\omega, k_h; z_0)} = \frac{\tilde{N}(z_0)}{\tilde{N}(z)} \sqrt{\frac{z_0 - z_s}{z - z_s}} \exp \left[-\frac{k_h^3}{\omega^4} \int_{z_0}^z \tilde{N}^4(z') \tilde{\nu}_{\text{tot}}^{\text{plume}}(z') (\tilde{N}^2(z') - \omega^2)^{-1/2} dz' \right]. \quad (1)$$

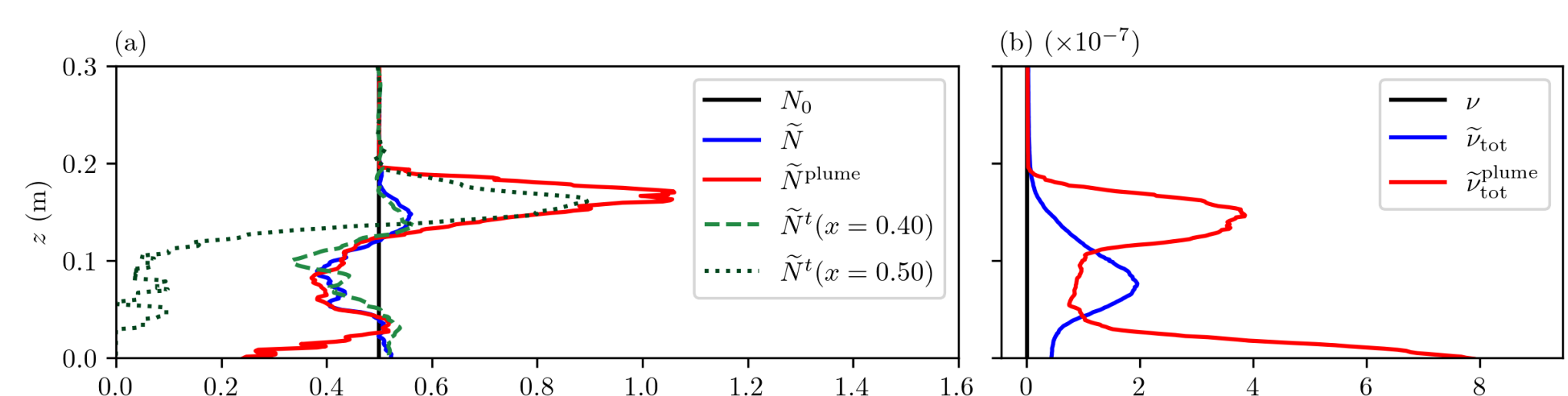


Figure 5. Vertical profiles of the time- and horizontal-average stratification strength \tilde{N}^{plume} (within the plume) and turbulent viscosity $\tilde{\nu}_{\text{tot}}$.

- Frequency spectra $P(\omega; z)$ are calculated from amplitudes $A(k_h, \omega; z)$ as $P(\omega; z) = \sqrt{\sum_{k_h} A(\omega, k_h; z)}$.
- The model sufficiently captures the power decay and frequency selection when initialised from a spectrum taken near the top of the fountain and assuming a source height within the fountain, near the intrusion. Discrepancies remain at low frequencies.
- The minimum decay rate in (1) given constant stratification and viscosity occurs at $\omega = \sqrt{4/5}N_0$.

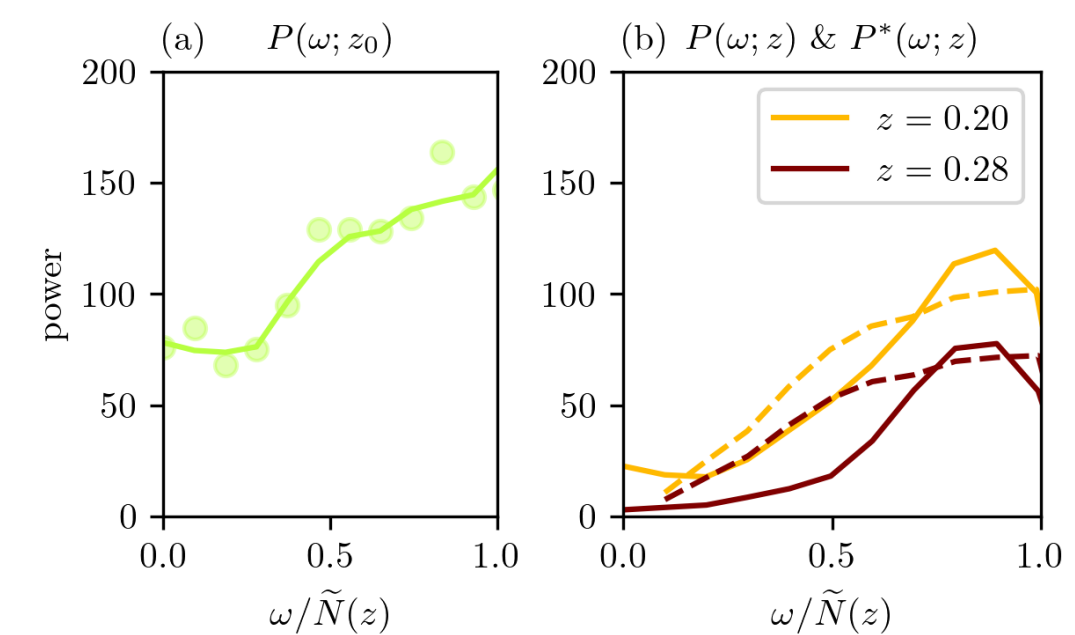


Figure 6. Example of viscous decay calculation. (a) Frequency spectrum at height $z_0 = 0.16 \text{ m}$ within the plume. (b) Predicted (dashed line) and actual (solid line) spectra above the plume.

Dynamic mode decomposition

- We use dynamic mode decomposition (DMD; Schmid (2010)) to extract spatial structures associated with specific frequencies. The modes are spatiotemporally coherent across the perturbation horizontal velocity u' , buoyancy b' , vertical velocity w' , and vorticity $\zeta_y = \partial_z u - \partial_x w$.
- 'Exact DMD' computes the eigen-decomposition of the linear operator that advances the data from one time step to the next.

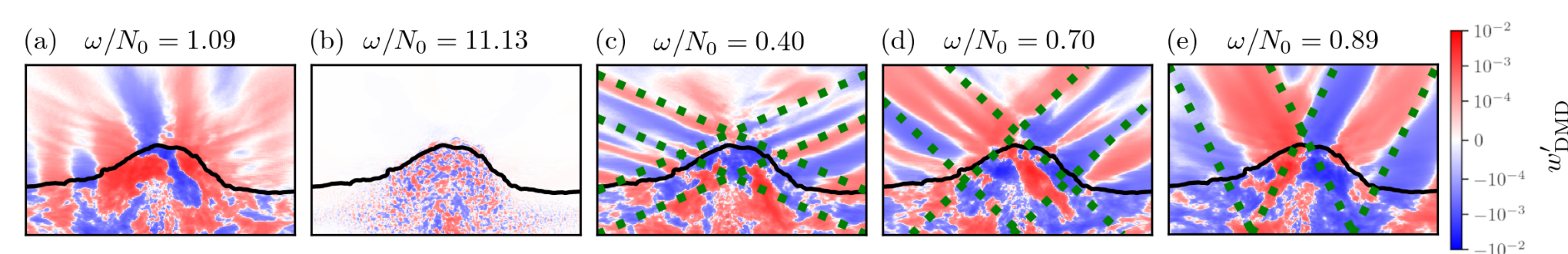


Figure 7. Examples of DMD modes. (a) Evanescent mode. (b) Turbulent mode. (c)–(e) Internal wave modes with theoretical phase angle in green.

- Finally, we use ray tracing on each DMD mode with an internal wave frequency $0 < \omega_{\text{DMD}}/N_0 < 1$. Rays are initialised at the source height $z_s = 0.12 \text{ m}$ used in figure 6. Rays are identified as 'coherent' wave beams where the phase is within $\pi/4$ of the mean phase along the ray.
- Coherent wave beams can be traced from inside the turbulent plume (figure 8).
- The method suffers from filtering artefacts and noisy data at the T/NT interface.

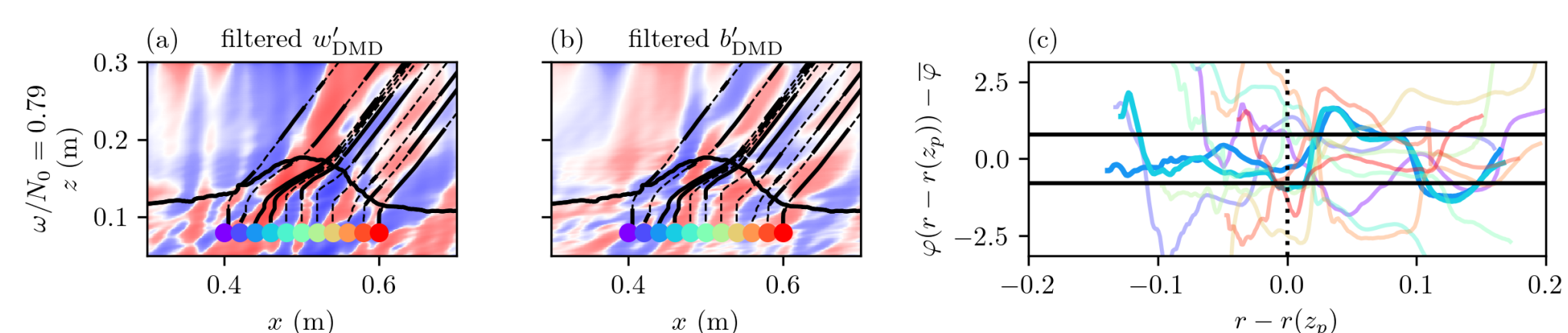


Figure 8. Example of ray tracing in a DMD mode, shown in (a) and (b). The phase along each ray is shown in (c) and emphasised in each panel where coherent.

Summary

- We use spectral analysis, a linear viscous decay model, DMD and ray tracing to show that internal waves generated by convective penetration of a stably stratified layer are formed within the turbulent plume.
- The wave spectrum is modified during propagation into the stratified environment. Understanding the generation mechanism remains an open problem.